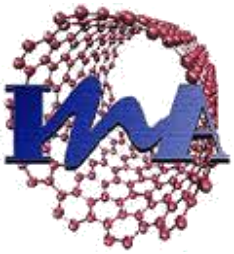

UNIVERSITY OF ZARAGOZA
Chemical Engineering and Environmental Technology Department

MICROPATTERNED SUBSTRATE MODIFIED WITH HYDROPHIC COATING FOR DEWATERING APPLICATIONS

Master´s Degree in Nanostructured Materials for Nanotechnology Applications

Author: Leidys Marleyn Rodríguez Castro
Tutor: María Pilar Pina Iritia
Tutor: Miguel Ángel Urbiztondo Castro
Enero 2013

My grateful and sincere thanks to Professors María Pilar Pina and Miguel A. Urbiztondo, for listening me at all moments, discussing with me and supervising all the details of this work.

I would like to thank scholarship program of the Fundación Carolina and University of Zaragoza for giving me the opportunity to develop my research in nanotechnology.

… To God and all my family

OUTLINE

LIST OF FIGURES

FIGURE

silicon support synthesized to 90°C by 20 hours.

LIST OF TABLES

TABLE

MICROPATTERNED SUBSTRATE MODIFIED WITH HYDROPHIC COATING FOR DEWATERING APPLICATIONS

1. INTRODUCTION

1.1. General description of zeolites.

A zeolite is a microporous crystalline aluminosilicate characterized by a three-dimensional framework structure with a system of channels and cavities permeable to molecules various. They are built up by various connections of TO_4 tetrahedra (T = Si, Al) with oxygen atoms connecting neighboring tetrahedra, at some places in the framework Al^{+3} has replaced Si^{+4} and the framework carries a negative charge loosely held cations that sit within the cavities preserve the electroneutrality of zeolite [1]. The zeolite composition can be best described as having three components:

$$M_{x/n}^{+n} \quad . \quad [Si_{1-n}Al_nO_2] \quad . \quad nH_2O$$

extraframework cations | framework | sorbed phase

Where M is a compensation cation of structure formed by the aluminosilicate , n is the cation valence, x and y represents the total number of tetrahedra per unit cell and w is the number of adsorbed water molecules in a single unit cell [2,3].

Depending on the structure, the size of the pores is in the range 3 to 13 Å (micropores i.e. d < 2 nm) [1]. Figure 1 shows the framework projections and the ring sizes for commonly studied frameworks. The crystalline nature of the framework ensures that the pore openings are uniform throughout the crystal and can readily discriminate against molecules with dimensional differences less than 1 Å, giving rise to the name "molecular sieves" which are structures able to separate molecules on size basis. Zeolite can adsorb a

remarkable variety of molecules of different size and therefore they can be utilized as sensible elements for the detection of a given molecular species. In fact it is selective adsorption, rather than molecular sieving, the mechanism that explains most of the successful gas separations achieved with zeolite membranes [4].

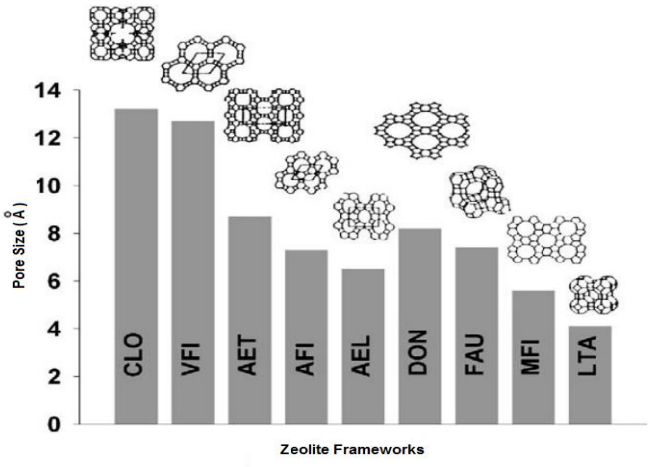

Figure 1: Comparison of pore sizes of different framework structures [2].

The framework topologies are represented by three capital letters, in accordance with the recommendations of the IUPAC committee on chemical nomenclature of zeolites. The Zeolite topology investigated in this work is zeolite A (LTA) and their structure is shown in Figure 2. An LTA-type zeolite is composed of equivalent amounts of Si and Al (Si/Al = 1). When a zeolite framework contains an equal number of aluminum and silicon atoms, each oxygen atom is linked to one aluminum and to one silicon atom, and the cavities contain the maximum density of exchangeable cations resulting in a high adsorption capacity [2,4]. The LTA-type structures is cubic with a three dimensional pore system. The free aperture diameter for the channel is 4.1 Å. Its three-dimensional channel system facilitates the diffusion of adsorbed molecules [5,6].

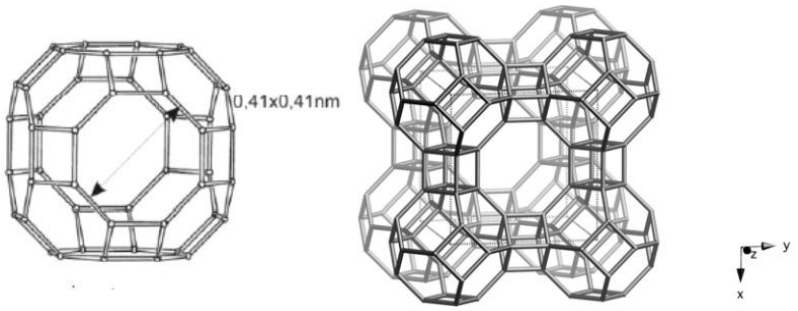

Figure 2: Structure and dimensional pore system for LTA zeolite. Framework viewed along [001]

1.2. Properties of zeolite and applicatons of micro-scale

In general, three main properties of zeolites are technologically important: they are selective and strong adsorbents, they are selective ion exchangers and they are catalytically active. All these properties give them a versatile potential for various applications such as separation, membrane reactors, chemical sensors, etc [7]. Their incorporation in the microdevices fabrication has been the focus of recent research: many-microdevices utilizing zeolites as host materials have been developed. Our group had developed several strategies for incorporating zeolites in miniature systems in base of structural and chemical properties of zeolites, using traditional semiconductor fabrication methodology; such as interdigital structures [8], cantilever based mass sensors [9,10], micromembranes [3] and microsensors [10-12]. The applications of this functional material for micro-devices fabrications, are based on morphology, quality, size and orientation crystal zeolite.

On the other hand, miniaturization implies a micro-size environment. It is very important to keep in mind that miniaturization is not only a decreasing of scale, but that other forces and phenomena are present in micro-size environments. In this sense, miniaturization offers funcitonal and economical benefits such as low reagent consumption, small (nanoliter) sample requirement, as well as, readiness for system integration and high throughput parallel processing, consequently leading to reduction in overall processing/analysis time, and sample contamination is minimizes by decreasing sample manipulations [13]. In other word, a miniature microfabricated chemical device offers unprecedented opportunity to control and manipulate the contact and mixing between well-defined fluid elements to attain a more efficient performance.

According to the written previously and in view of their multiple properties, specially selective adsorption properties, and variety of applications , it is not surprising that zeolites have used in a number of works dealing with gas sensing micro-devices, either as an adsorption target or as a barrier to prevent the adsorption of interfering molecules [14]. However, miniaturized gas sensors/detectors typically have limited performance for accurately detecting analyte (trace gas) with small concentration levels at the ppb (parts-per-billion) range. The detector errors arise primarily from carrier (diluent) gas interference and high noise to signal ratios [15]. A preconcentrator incorporated at the front end of an miniaturized gas analysis system can enhance the overall performance of the system. A preconcentrator is an analytical devices and consists basically, of an adsorbent material placed on a heating support [15,16]. The nature of the adsorbing material is the most important parameter determining the performance of the gas [17], also structure (from planar to 3D), desing and operating parameters.

1.3. General about µ-preconcentrators

The preconcentration process consists in adsorbing the target gas at room temperature on a specific adsorbent as zeolite, over a time period necessary for to concentrate the chemical compound into the adsorbent. After analyte-collection phase is complete, the thermal desorption is next step allowing to generate a higher concentration of the target compound to the connecting detectors (e.g. gas sensors, electronic nose or conventional analytical detectors such as gas chromatograph/mass spectrometers, etc). The gas micro-preconcentrator lowers the detection limit of the system and improves detection sensitivity smaller concentrations (at ppb or ppt levels).

The fundamental mechanism behind preconcentration is physical adsorption or physisorption, this phenomenon involves weak intermolecular forces between the gaseous phase, called the adsorbate, and the solid surface, termed the adsorbent, that are easily reversed [15]. During extraction at room temperature, the adsorption of target analyte occurs only on the surface of a adsorbent and this phenomenon depends on surface

properties and the amount of surface available for adsorption. In the desorption process, the adsorbate flies off the adsorbent because the high thermal desorption temperature imparts kinetic energy to the adsorbates to escape the adsorbent. However, this temperature must be adjusted so as not to cause a thermal decomposition of the target analyte.

Conventional pre-concentrators, so called microtraps, appeared in the 1970s for air sampling applications [18-20]. They generally comprise a stainless steel or glass-capillary tube or glass-capillary tube packed with one or more granular absorbent materials. For desorption, current is passed through the stainless-steel tube or through a metal wire coiled around the glass-capillary tube. These devices have been used are large in size (several centimeters in length and few millimeters to 1 centimeter inner diameter) and consume high power during thermal desorption. They also suffer from limited heating efficiency due to their large thermal mass. Since then, many works have been carried out: preconcentrators with different geometries and materials such as microchannel onto glass support [21], micro-spiral and microcapillars on silicon substrate [22,23], Plate of polymers (SU8) [24], tube of stainless steel [25], alumina supports [26], etc.

Miniaturized or microfabricated preconcentrator devices have been reported commonly into two categories: structures planar or 3D microconcentrators. The planar microhotplate structure could be a simpler fabrication option. However, the amount material concentrated with this structure is generally lower than 3D based pre-concentrators, because of the lower amount of absorbing material which it could host [15]. Ivanov and co-workers, developed a 3D micro preconcentrator which consists of a spiral-shaped fabricated with silicon technology for bencene preconcentrations. Pijolat et al. presented the development of a gas preconcentrator based on a micro-channel in porous silicon filled with carbon nanopowders by a micro-fluidic process [27] . Silicon is an ideal structural material for this application because of its electrical, mechanical, and thermal properties. On the other hand, the photoresin SU-8 is an epoxy-based photosensitive polymer designed for micromachining and other microelectronic applications where a thick chemically and thermally stable image is desired [28]. In desing of preconcentrator is used as material support, ideally suited to

the fabrication of micro-channels for micro fluidic and bioMEMS devices. Grzelka et al. used a preconcentrator with SU-8 technology for analysis of different kinds of cells/microparticles.

The adsorption capacity of the preconcentrator is a critical issue in the design and operation of the preconcentrator and it governs the minimum size of the microdevice. The selection of the adsorption materials is mainly based on experimental characterization of the adsorbents and their behavior with the target gases molecules [17]. zeolite can be an interesting candidate for preconcentration applications because have a good selectivity due to their homogeneous pore size, moreover exhibit a high thermal stability, high resistance to corrosive gases and strong adsorption affinity allowing the capture of gases at very low concentration. Indeed, zeolites are capable of separating molecules by their size, shape and polarity. Moreover, zeolite coatings and films have been successfully grown on flat and micropatterned substrates using various synthesis approaches [3-5,12]. This enabled to Lahlou et al, the incorporation of zeolites (i.e., FAU) as adsorbent potential in a 3D micro-preconcentrator for analysis of orthonitrotoluene. The ability to grow a stable of zeolite film in a desired area is a critical issue to their use in micropreconcentration. A zeolite coating/film with high quality can be fabricated by using zeolite nanocrystals as building blocks [29].

1.4. Zeolites crystallization

Zeolite synthesis involves the hydrothermal crystallization of active hydrated aluminosilicate gels or sols in a basic environment. The gel is defined as an aqueous solution containing a silica source, an aluminum source and an alkali source. Hydrothermal synthesis usually refers to reactions occurring under conditions of high temperature–high pressure (>100 ºC, >1 bar) in a closed system (Figure 3) [7]. The duration required for crystallization varies from a few hours to several days. The general factors influencing hydrothermal zeolite synthesis are well known (reactant sources, Si/Al ratio, alkalinity, water content, inorganic cations, organic templates, solvents, temperature, aging, stirring, and seeding) [29].

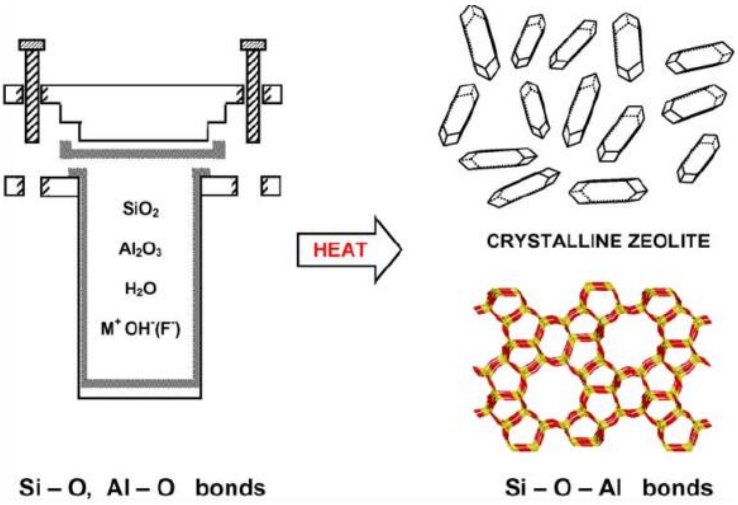

Figure 3. Hydrothermal zeolite synthesis. The precursor materials are converted into the crystalline product whose microporosity is defined by the crystal structure. During the hydrothermal reaction in the presence of a ‘‘mineralising’’ agent (most commonly an alkali metal hydroxide), the crystalline zeolite product (e.g. zeolite A) containing Si-O-Al linkages is created.

Basically, the hydrothermal synthesis procedure can be ex situ and in situ methods (figure 4), that is with and without a previous seeding step. The in situ hydrothermal synthesis is method in which the support is immersed into the synthesis solution and the layer/film is formed by direct crystallization. Coating the zeolite seed on the support surface before hydrothermal synthesis, which is also called a secondary growth method (ex situ), is an effective approach to develop a high-quality zeolite coatings.

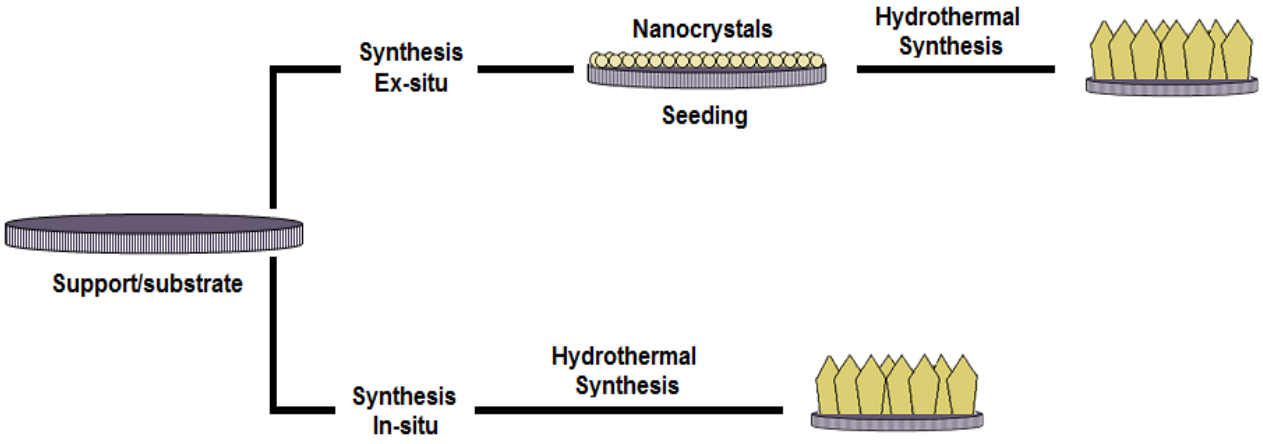

Figure 4. Two possibilities for synthesis of zeolite polycrystalline layers. Mode ex-situ or in-situ

2. AIM OF THIS WORK

This work is part of the research line focused in developing microsystems with layers/coatings zeolitic as a hallmark. Therefore, A-type zeolite has been investigated for its potential use as adsorbent material for to create micro-traps/micro-preconcentrators of water in gas streams. In order to accomplish this objective, next steps have been followed:

- The first part of this work was aimed at the optimization of method for deposition and intergrowth of coating/films A-type zeolite defect-free onto silicon dioxide wafer (flat substrate), since previous work by our group demonstrated that the main problem associated with zeolite coating synthesis is crack formation,

- In the second part, was devoted to seeding the microchannels fabricated on silicon oxide and photoresin SU-8 support with A-type zeolites enabling the deposition and growth of defect-free zeolite film by hydrothermal synthesis in the case of silicon substrate.

- In the end, we have evaluated the possibility of preconcentration on microchannels for water/nitrogen in gas stream, through analysis adsorption/desorption of seed A-type zeolite, nanocrystal zeolite A and coatings onto silicon plane substrates.

3. EXPERIMENTAL

The zeolite layers characterized in this work were prepared according to the method described by previous work [30]. Basically the deposition of zeolite LTA layer onto the substrate involves two main steps, namely seeding and hydrothermal growth. In the first step, seeding process, the surface of silicon oxide support is modified in order to promote the adhesion of colloidal zeolite seeds, oppositely charged. The surface of the substrate was modified by reacting with two different compounds: an cationic polymer, poly(diallyldimethylammonium chloride) (PDDA) and Boehmite, an aluminium oxide hydroxide (γ-AlOOH) mineral. A zeolite nanocrystals colloidal solution with a concentration of the solid nanocrystals of 2 wt% was spread and spinned onto modified support. The seeded support is then hydrothermally treated in the same synthesis solution to allow the growth of zeolite seeds into a dense film.

The directed growth of zeolite A within the confined space of microfabricated channels on silicon dioxide substrates has been developed in the second part of this work. The surface of the substrate was modified by reacting with Boehmite (shows better results than the PDDA). Following, the seeding processes and hydrothermal synthesis were carried out. Finally, the incorporation of zeolite seeds on micro-channel of SU-8 resin was realized by seeding continuous flow process, with a volumetric flow 0,1 mL/min. The SU-8 support was modified with PDDA covalent linker. The microchannels in SU-8 resin cannot undergo hydrothermal synthesis due to the instability of the material at the temperature for zeolite synthesis.

3.1. Preparation of zeolite LTA seeds

The A nano-zeolite seeds were prepared by hydrothermal synthesis according to the procedure reported in a previous work by the authors [3,12,30]. In a typical preparation of 100 g of zeolite seed, 12.78 g of LUDOX (AS-30 Aldrich) were diluted in 11.36 g of DDI water in a polypropylene vessel and stirred at room temperature until completely dissolved

(solution 1). In a separate vessel, 4.26 g of aluminum isopropoxide ($C_9H_{21}O_3Al_3$ 98 wt % Aldrich), 28.4 g of Tetramethylammonium hydroxide pentahydrate ($TMAOH.5H_2O$ 97 wt% Sigma Aldrich), 39.76 g of DDI water and 3.4 g of 1M sodium hydroxide (NaOH97 wt% Sigma Aldrich) solution were combined and stirred during 1 h until completely dissolved (solution 2). Finally, solution 2 was added to solution 1 under stirring during 48 h, at room temperature, until homogeneous dissolution, then transferred to a polypropylene bottle and heated to 100°C in rotary evaporator for 15 h under static conditions.

The final mixture having a molar composition of $13.4(TMA)_2O:0.3Na_2O:1.8Al_2O_3:11.25SiO_2:700H_2O$. The zeolite product was then washed with deionized water and dispersed in DDI H_2O, and then it was centrifuged at 10.000 r.p.m. for 30 min and redispersed in DDI H_2O again under ultrasonic bath. The washing procedure was repeated several times obtaining a final dispersion of nanocrystals seeds at pH 10.

3.2. Preparation and fabrication of zeolite composite substrate

3.2.1. *Preparation of flat and 3D substrates.*

The flat substrates used for the preparation of the zeolite-silicon composites were commercial 3 inch silicon wafers with a <100> crystal orientation. These silicon wafers were thermally oxidized at 1000°C in order to obtain silicon oxidized wafers with a SiO_2 thickness of 700 nm. A tubular oven (Carbolite) has been used for growing thermal SiO_2 layers onto silicon wafers . We have used two different processes: dry oxidation, using O_2 and N_2 , and wet oxidation, bubbling O_2 and N_2 through DDI water. The usual procedure is to grow a mixed oxide sandwich: dry oxidation + wet oxidation + dry oxidation. The water required for the wet oxidation is achieved by saturating the input stream of oxygen through a bubbler to 100 °C. The process variables are oxidant gas composition and the oven temperature. Before seeding process, silicon oxide substrates were sonicated in acetone for 10 min, a mixture of acetone (50%) and ethanol (50%) for others 10 min, and rinsed with a copious amount of deionized water. After that, silicon oxide wafers were cleaned in freshly prepared Piranha solution (a mixture of 30% H_2O_2 (35% wt% Sigma Aldrich) and 70% of

H_2SO_4 (96 wt% Panreac)) for at least 0.5 h, rinsed exhaustively with deionized water, and dried in a stream of nitrogen gas.

On the other hand, the 3D-substrates (microchannels) were fabricated onto silicon wafers using the following procedure. A thick layer of polymer resist (AZ 6624) was spin-coated onto the silicon oxide wafer, and micropatterned using standard photolithography techniques. The schematic drawing in figure 5 illustrates the procedure for the fabrication of microchannel onto silicon wafer. After exposure the wafers to ultra violet light for final pattern transfer, the support was attacked with strong alkaline substances (pH > 12) such as aqueous KOH or $TMAH^-$ solutions (Anisotropic Silicon Etching)

$$Si + 4OH^- \longrightarrow Si(OH)_4 + 4e^-$$

Since the bonding energy of Si atoms is different for each crystal plane, and KOH/TMAH Si etching is not diffusion- but etch rate limited, Si etching is highly anisotropic: the (100)-orientated wafers form square-based pyramids with (111) surfaces. Finally, silicon wafers were again thermally oxidized and the microchannels were seeded with zeolite A.

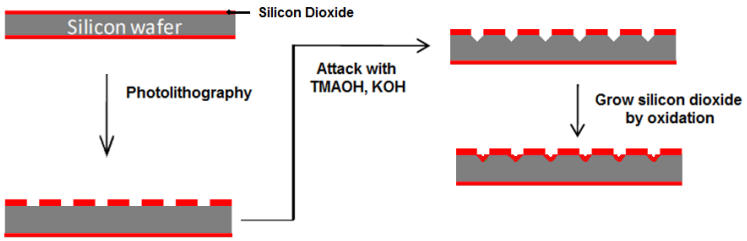

Figure 5. Process flow for the fabrication of microchannels onto silicon support.

The patterns, shown in figure 6, consists of 60 (Fig. 6a) and 47 (Fig. 6d) microchannels with a length of 3,66 and 5 μm respectively and line spacing of 50μm approximately into the plate with area of 1 cm^2. The channels measuring around 50 μm wide and 38 μm deep. The pattern was coated with Boehmite onto which was adsorbed a layer of nanometer sized zeolite seeds (i.e., 90.8 nm). A layer of a-type zeolite film was grown onto the seeded pattern following hydrothermal synthesis at 90°C for 7,5 h. A Teflon-lined stainless steel autoclave with a reactor volume of 35 cm^3 was used in the zeolite crystallization and growth.

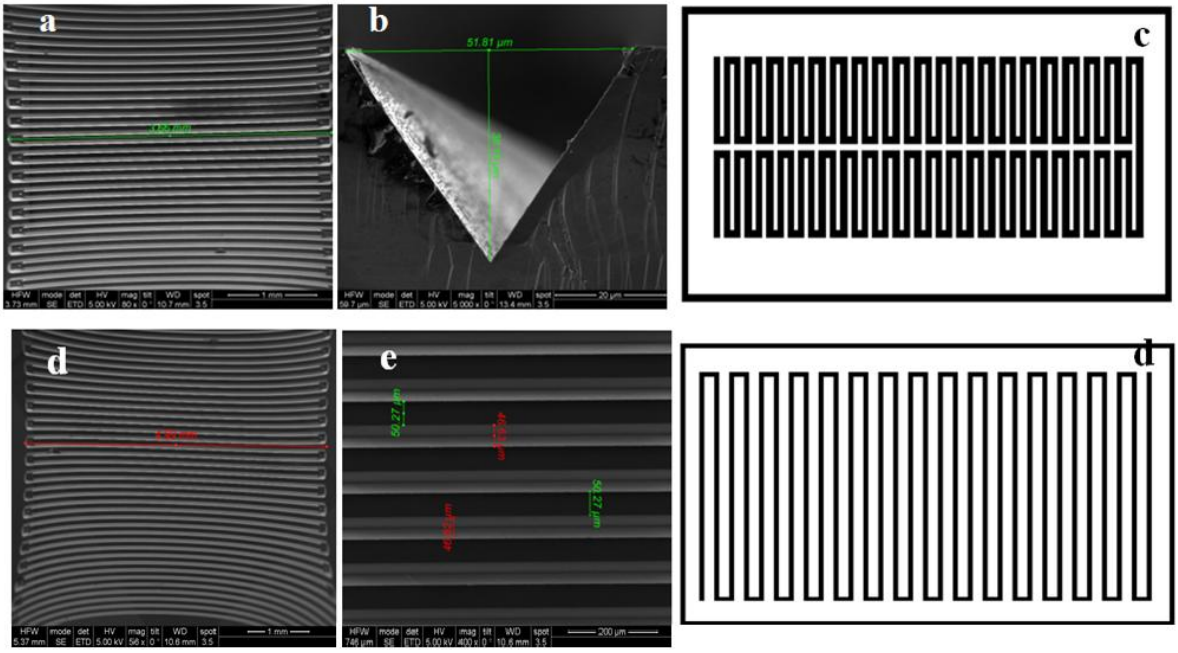

Figure 6. Scanning electron microscopic images of the microchannels on silicon wafer: (a),(d) Top view two different patterns, (e) prospective view, (b) cross-section and (c),(d) The microchannel patterns.

Refer to figure 7 below for step-by-step pattern transfer and etching of the channels mask the cross-sectional of the SU-8 substrate. The etch process began with deposition of a layer of phothoresin SU-8 onto kapton support. To apply the pattern of the channels to the SU-8 layers, the contact photolithography of the channels mask was performed using an SÜSS MICROTEC MA6 model Series Mask Aligner, the channels mask was aligned over the front-side of the coated SU-8 substrate. The support were then exposed to ultra violet light for final pattern transfer, after deposition of a second SU-8 layer. Figure 8 illustrates of images of the microchannels fabricated in SU-8 resin. and microdevices used for the seeding process. The channels measuring around 100 µm wide and 100 µm deep.

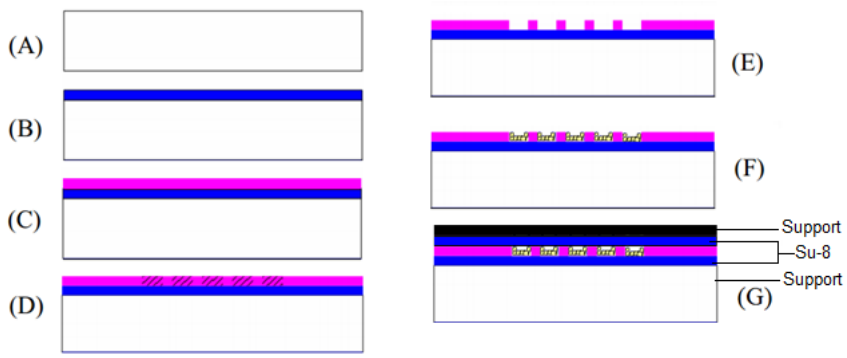

Figure 7. Photolithography of microchannels mask. A) Clean Kapton support, B) spin photoresist of first layer and cured. C) spin photoresist osf second layer, D) expose Channels mask, E) develop, F) seeding process G) microdevice closed

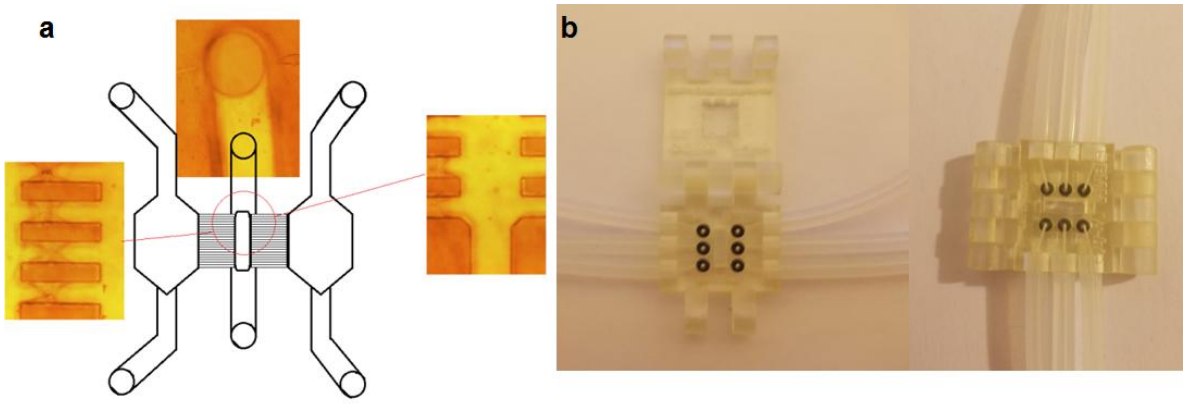

Figure 8. a) Microchannels pattern on SU-8 resin, b) microdevices for seeding process of microchannels fabricated in SU-8 resin

3.2.2. *Seeding process zeolite A*

Surface seeding accelerates the zeolite crystallization process on the support surface, and also enhances the formation of homogeneous zeolite A layer. But the main problem associated with coating synthesis is crack formation. In previous works in this research group have used PDDA as covalent linker between zeolite seed and silicon support however, forming cracks in the coatings zeolitic cannot be avoided. Formation of crack was reduced by applying intermediate layer, between the support surface and seed layer

The linkers PDDA and Boehmite adsorbed on the support surface are used to capture LTA zeolite particles during hydrothermal synthesis. It is expected that because of the electrostatic interaction, the negatively charged LTA zeolite particles can homogenously and easily migrate to the positively charged support surface, facilitating the formation of a uniform and dense zeolite LTA layer. The preparation scheme is shown in Figure 9.

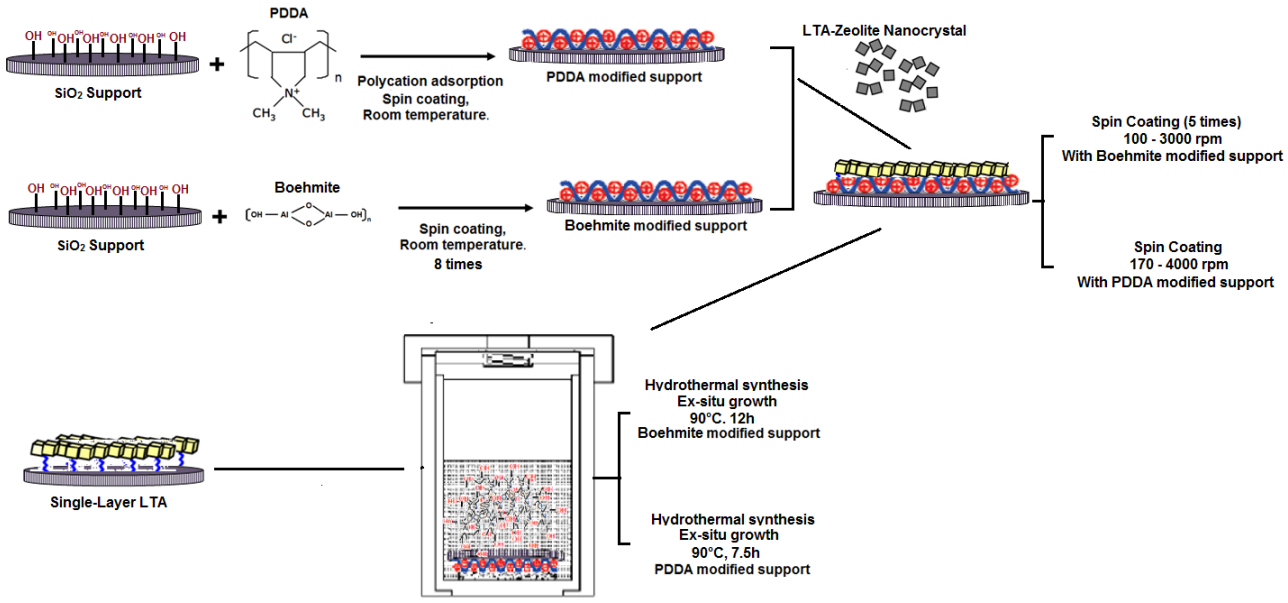

Figure 9. Scheme of the hydrothermal synthesis of a zeolite layer using poly(diallyldimethylammonium chloride) (PDDA) or Boehmite as interlayer. In the first step, the support was modified by PDDA and Boehmite, following seeding steps and finally, hydrothermal synthesis.

Cationic polymer, poly(diallyldimethylammonium chloride) ($(C_8H_{16}ClN)_n$ 20 wt% in water Aldrich), was deposited on the substrates prepared as above. The solution of PDDA was prepared solving 1.47 g of NaCl (99 wt% Panreac) and 0.25 g of PDDA in 50 ml of DDI water, the solution was stirred till completely dissolve the poly(diallyldimethylamonium) chloride and after the solution was spinned onto the silicon substrate. Finally, the silicon substrate was seeded with zeolite nanocrystals before hydrothermal synthesis. The colloidal solution seeds of zeolite spread and spinned onto the substrate. The angular speed used was initially 170 r.p.m by 1.5 minutes, to spread all the deposited material onto the substrate and then was spinned at 4000 r.p.m by 2 minutes, in order to finish the covering and evaporate the solvent. These parameters reproduce the optimal conditions reported by

previous work [30]. The use of PDDA allows reversing the charge of the SiO_2 surface in order to obtain a positively charged substrate and produce attractive electrostatic interactions between the surface of the substrate and the zeolite nanocrystals, as shown in figure 9. PDDA is always cationic, regardless of pH.

The modified support were coated with LTA-type zeolite crystals as nucleation seed. To get a uniform layer on the support surface, the nucleation seeds should be very small and uniform in size. The particle size of seed crystals was 90.8 nm (average particle size measured from SEM and DLS). In order to get a uniform seed layer on the support surface, the seeds should be dispersed homogeneously on the support surface. In this seeds coating process, the support substrate was spinned with a 2 wt% LTA-type zeolite suspension in deionized water 5 times for a duration of 1 minute at 100 r.p.m for to thin the fluid and then 0.5 minute at 3000 r.p.m for to eliminate excess solvents from the resulting film. After the spinning procedure, the seeded supports were dried at 150°C for 24 h. The zeolite A layer were synthesized hydrothermally on silicon dioxide modified, seeded support wafer.

A typical spin process consists of a dispense step in which the material is deposited onto the substrate surface, a high speed spin step to thin the fluid, and a drying step to eliminate excess solvents from the resulting film. Figure 10 shows an schematic description of the followed spin coating process.

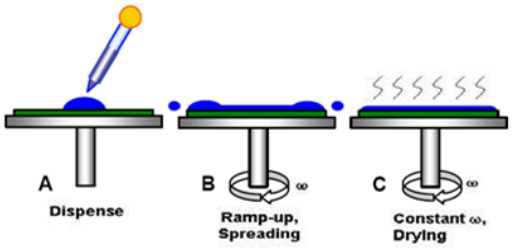

Figure 10. Spin-coating process. Dispensing of solution (A). Distribution (B). Uniform thinning (the solvent evaporation).

Boehmite nanoparticles were prepared by a peptization method according to a procedure developed by Yoldas [31] Twenty five grams of aluminum tri-sec-butoxide $Al[OCH(CH_3)C_2H_5]_3$, 97 wt% Aldrich) precursor was hydrolyzed in 100 mL of distilled water at 80°C for 1 h, under vigorous stirring to form a white precipitate. Then 7 mL of

nitric acid (HNO_3, 64-66 wt% Aldrich) was added and the temperature raised to 90 °C and maintained at this level for 20 h. At the end of this process, a sol containing boehmite AlO(OH) in 9 wt% is obtained. The boehmite layer was applied by spin coating method. Initially the boehmite solution was spinned onto silicon dioxide wafer. Spinning time was of 1 minute at 100 r.p.m followed by 0.5 minute at 3000 rpm and repeated 8 times. Then, the substrate was dried at 200 °C for 2h. A thin layer of boehmite was formed on support surface.

The structural element in boehmite crystals consists of double chain of AlO_6 octahedra giving double molecules. These chains are parallel, forming layers with OH group outside. These hydroxyl groups will form hydrogen bonds between hydroxyl ion and neighboring group. Therefore, an increase in hydroxyl group density causes a better attachment between the zeolite and the support. Figure 11 presents a parallelepiped model of the nano-sized boehmite slabs, showing clearly the importance of the hydrogen-bonded layers.

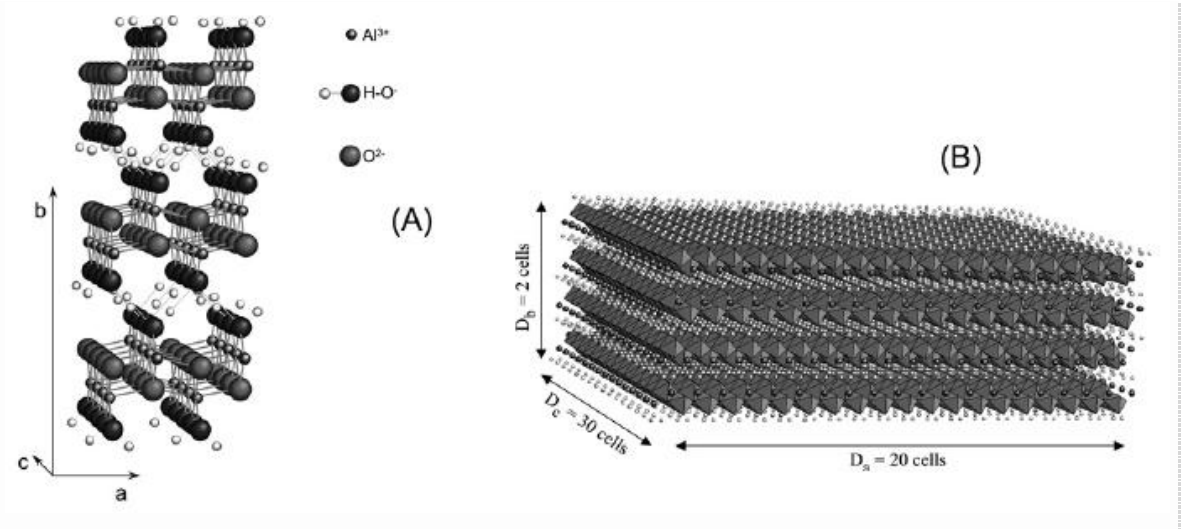

Figure 11. (A) Boehmite structure and unit cell. (B) Boehmite model of nano-sized boehmite crystallites.

In the case of microchannels on silicon substrate, the boehmite layer was applied by dip coating method. Dip coating is a simple process for depositing a thin film of solution onto a plate, cylinder, or irregular shaped object [3]. The fact that the geometry of the substrates can vary widely is a distinguishing feature of the dip-coating technique. In a dip-coating process, a substrate is dipped into a liquid coating solution for some time thereby ensuring that the substrate is completely wetted, and then is withdrawn vertically from the solution

bath with a well-defined withdrawal speed under controlled temperature and atmospheric conditions. The coating thickness is mainly defined by the withdrawal speed, by the solid content and the viscosity of the liquid. The liquid film formation is achieved by two main mechanisms, i.e. gravity draining of liquid solution and evaporation of solvent. This deposition technique has been combined with the layer by layer assembly technique in order to obtain a better coverage of the substrate. Figure 12 shows an schematic description of dip-coating process.

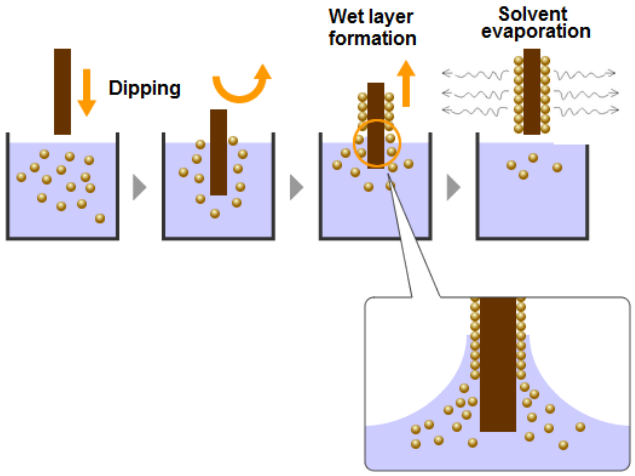

Figure 12. Stages of the dip coating process: dipping of the substrate into the coating solution, wet layer formation by withdrawing the substrate and gelation of the layer by solvent evaporation.

Initially the microchannels on silicon dioxide substrate were dipped into boehmite sol. Dipping speed was 0.1 mL/s and repeated 5 times. Then, the substrate was dried at 200°C for 2 h. A thin layer of boehmite was formed on support surface. The modified support was coated with A zeolite crystals as nucleation seed. In this nucleation seeds coating process, the support substrate was dipped in a 1 wt% of A-type zeolite suspension in deionized water 5 times with a dipping speed of 0,1 mL/s. After the dipping procedure, the seeded supports were dried at 150.C for 24 h. The schematic drawing in figure 13 illustrates the procedure for the fabrication of microchannel with zeolite layer.

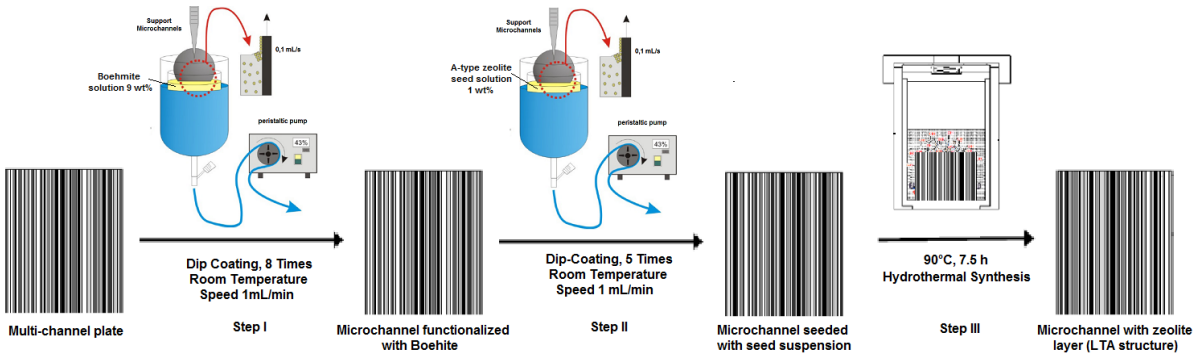

Figure 13. Fabrication of microchannel pattern with zeolite layer: It involves the grafting of Boehmite on the microchannel wall (step I) followed by the attachment of nano-zeolite seeds (step II). The microchannel plate was immersed in solution hydrothermal synthesis (step III).

The seeding process inside michochannel of resin SU-8 was carried out according to the procedure described as follows and whose general form is illustrated in figure 14. In first step a PDDA solution (0.25 g of PDDA in 50 ml of DDI) were constantly pumped into the microchannel inlets using a peristaltic pump (Aglent 1Fs) at flow rate of 0.1 mL/min by 1 hour, changing the direction of flow for periods of 10 minutes. The second step, zeolite seeds were conducted into microchannel devices with the same conditiones described as above, concentration of zeolite seed was 1 wt%. Finally microdevice was dried at room temperature.

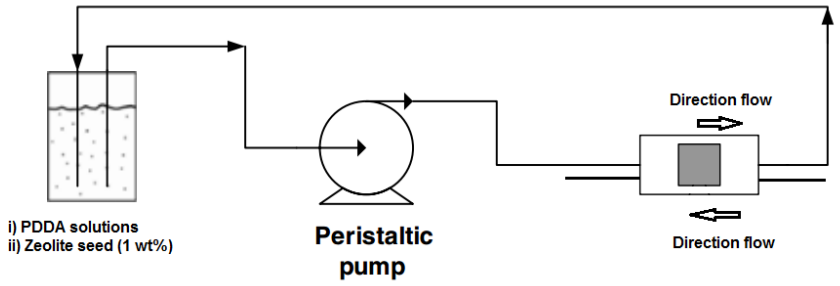

Figure 14. Schematic of experimental flow loop used in microchannel

3.2.3. *Hydrothermal Synthesis of layer A-type zeolite.*

LTA-type zeolite layer onto silicon dioxide wafer was synthesized according to the procedure described in a pevious work [35,39] as follows. A gel having the following molar

composition: $2.8Na_2O:2.7SiO_2:1Al_2O_3:174\text{-}347H_2O:0.05(TMA)_2$ was prepared using LUDOX AS-30 as the silica source and sodium aluminate (AlO_2Na Quimivita) as the Al source. A typical preparation involved combining 0.9052 g NaOH, 0.2719 g of Tetramethylammonium hydroxide (TMAOH) and 2,7833g of sodium aluminate in 40 g of DDI water with stirring. At the same time, 8.1045 g LUDOX AS-30 were mixed with 47.9347 g water and stirred. After aging each mixture separately for 1 h, the two mixtures were mixed slowly under stirring at room temperature. The resulting mixture was stirred vigorously for 18 hours to produce a homogeneous gel, followed the seeded wafer was placed in a horizontal position with the seeded surface facing downwards in the synthesis solution and during hydrothermal synthesis in a Teflon-lined autoclave at 90°C for 7.5 h under static conditions for modified support with PDDA and 12 h for modified support with Boehmite. A Teflon-lined stainless steel autoclave with a reactor volume of 850 cm^3 was used in the zeolite crystallization and growth. The resulting LTA-type zeolite layers was washed with deionized water and dried at 150°C in air for 24 hours.

3.3. Adsorption/desorption analysis

Adsorption/desorption measurements were carried out using thermal gravimetric analyzer (TA Instrument, TGA:Q5000) the experimental setup shown in figure 15. Thermogravimetric analysis is simply the determination of the mass of a sample as a function of temperature. A sample is placed into a crucible on a sensitive microbalance. The crucible is surrounded by a computer controlled oven. A flowing stream of gas allows the background atmosphere to be controlled. To avoid oxidation of the sample, the gas chosen is N_2. High-resolution thermogravimetric analysis (TGA) was used to estimate the absorbate concentration in the starting sample and to compare the changes induced in the weight of adsorbent during analysis.

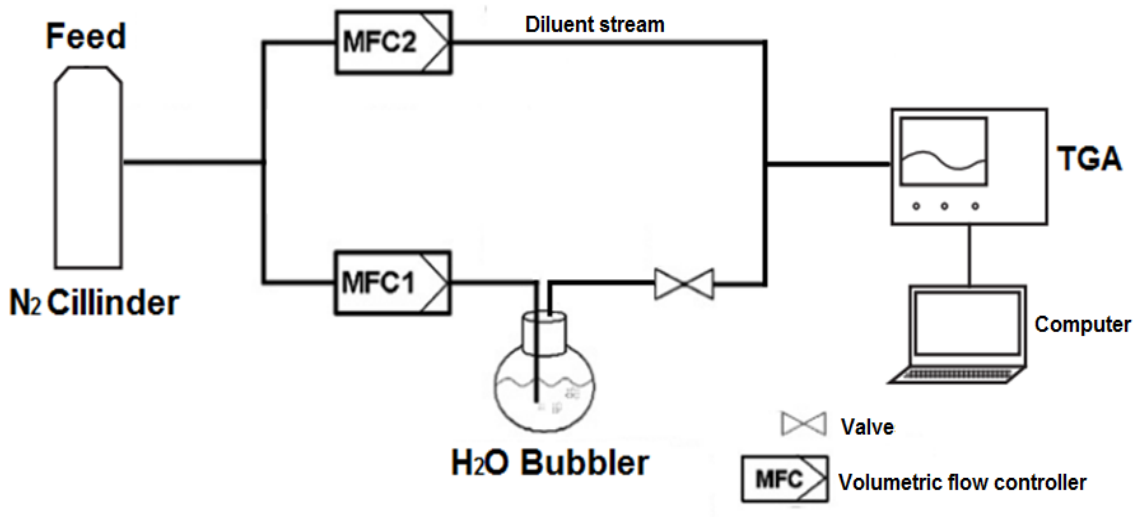

Figure 15. Schematic diagram of the experimental setup adsorption/desorption analysis.

In a typical experiment, the sample was first dried at 200 °C for 2 hours with thermal ramp rate up of 5 °C/min in a flowing nitrogen atmosphere. Nitrogen was used as purge gas, carrier gas, and as the diluting agent. Total carrier and dilute gas flow was 40 mL/min in order to avoid capillary condensation. Following, the sample was cooled until reach to equilibrium at 40°C. Then, a certain amount of hydrated material (gas stream N_2/H_2O) was quickly loaded into experimental setup and it was passed through the sample, providing good contact between the solid and the adsorbate. As adsorption occurred in the sample, its mass changed. The system measures small changes in the mass of adsorbent while steady flow of gas passes through it. Steady state was ensured by waiting at least 2 h prior to sampling data.

Adsorption isotherms were obtained for the gas stream N_2/H_2O mixture and the three samples (Zeolite seeds, zeolite nanocrystals, and zeolite layer intergrown on silicon dioxide substrate) at constant temperature and pressure . The adsorbate was introduced into the system by gas through a saturator containing water. The flow of N_2/H_2O was measured employing a pressure of 1.5 bar on the side of the feed. The partial pressure of the adsorptive in the gas stream going through the sample was controlled by mixing the carrier gas with the diluent (Nitrogen) stream. The composition of mixture gasses was 10000 ppm. The temperature of the saturator was maintained at room temperature (20 °C

approximately). In these experiments adsorbent samples of interest were calcined at 480 °C by 8 hour and with thermal ramp rate of 1 °C/min in order to eliminate of template ($TMAH^-$).

Following adsorption analysis, the temperature was increased gradually according to a preset program (usually 5 °C/min) up to 200 °C and dry nitrogen was introduced, immediately the weight of sample changed due the desorption of water, which changed the mass of the sample. The adsorption, desorption and analysis steps can be performed at the same run automatically.

3.4. Sample characterization.

The surface microstructure and morphology before and after hydrothermal synthesis was characterized by Scanning Electron Microscopy (SEM) using a INSPECT FEI Model operated at 5 kV. The chemical composition (Si/Al ratio) of crystal zeolite and layer zeolite was determinated by EDX (Energy-disperse X-ray spectroscopy) (INCA Oxford Instruments). The layer thickness was estimated with the same technique by investigating perpendicular fracture surfaces. The average seed size of zeolite was estimated via Dynamic light scattering (DLS: Brookhaven Instrument 90 Plus) for determine the size distribution profile of seeds in suspension and the average seed size deposited onto supports was characterized by scanning electron microscope. The characterization of boehmite is carried out by X-ray diffraction (XRD), IR spectroscopy and the morphology was evaluated by Transmission Electron Microscopy (TEM) using TECNAI T20 Model operated at 200 kV and LaB6. X-ray diffraction analysis was performed using a Rigaku/Max. The IR spectra have been measured with a equipment VERTEX 70 with a holder MIKI Goden Gate ATR, in the range 4000 - 600cm^{-1} and a band resolution of 5 cm^{-1}.

4. RESULTS AND DISCUSSION

4.1. Synthesis of LTA-zeolite seeds

4.1.1 *Morphology and average seed size.*

Synthesis of zeolite A nanocrystals were prepared as described above. The morphology of the nanocrystals obtained and the particle size deposited onto silicon dioxide wafer were characterized via Scanning Electron Microscopy. Dynamic Light Scattering was used in order to obtain the particle size distribution in suspension. Results obtained from the SEM image fit with the results obtained from DLS. Two different populations are observed with DLS technique for the synthesis 48 hours of aging time and 15 hours of synthesis time, one of around 108,4 nm and the other of 17,1 nm. The average crystal size, reported by DLS, was~90,8 nm and the polydispersity index was 0,16. As the value of the polydispersity index is significantly larger than 0,2 and the calculated hydrodynamic radius is no longer reliable. Figure 16 and 17 shows SEM images and DLS results, respectively, for the nanocrystals obtained. Figure 16 (b) shows the SEM image of zeolite seeds deposited onto silicon dioxide support modified with boehmite solution (9 wt%). The seeds have a typical cubic form from the LTA zeolite. Figure 17 show DLS results for the nanocrystals obtained.

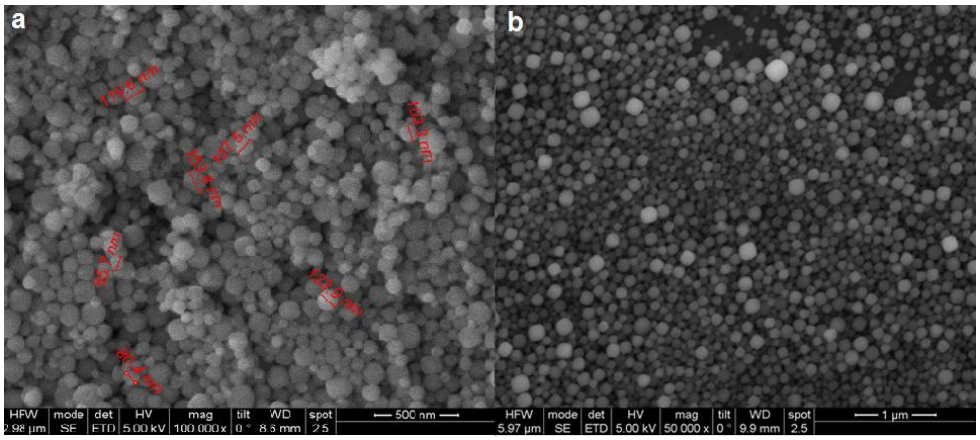

Figure 16. SEM micrographs of Na-A zeolite synthesized from 13.4$(TMA)_2O$:0.3Na_2O:1.8Al_2O_3: 11.25SiO_2:700H_2O and 100°C for 15 h a) Particle size b) Morphology of zeolite seed.

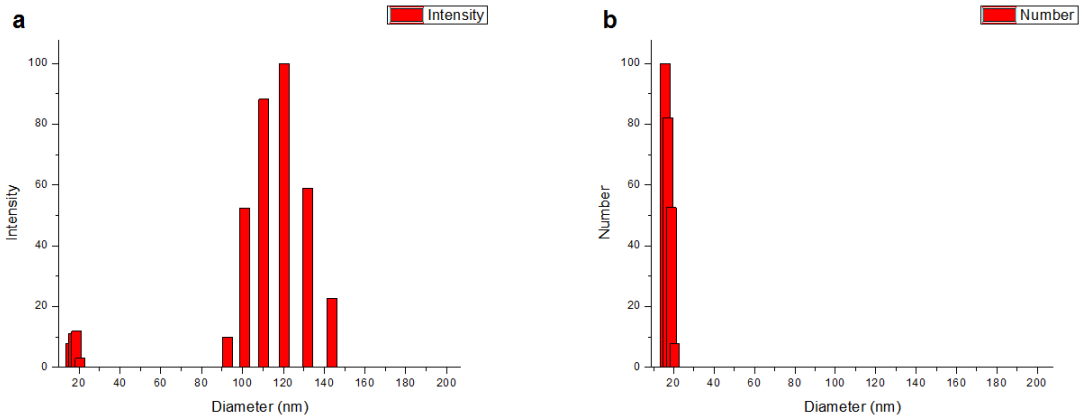

Figure 17: DLS of zeolite A nanocrystals obtained from 13.4$(TMA)_2O$:0.3Na_2O:1.8Al_2O_3: 11.25SiO_2:700H_2O.and 100°C for 15 h a) Mean Diam~108,4 nm b) Mean Diam ~17.1 nm

4.1.2. *The chemical composition*

Chemical composition of the as-synthesized nano zeolite seed can be found in Table 1. EDX-SEM results show that the synthesized product only contained Silicon, Aluminum, Sodium and Oxygen atoms. The Si/Al ratio of the as-synthesized zeolite was 1.57, which is in the reported range of zeolite A compositions. Using of template in the synthesis of zeolites tends to change the Si/Al ratio of the final products. For example, zeolite A, synthesized by using template (tetramethylammonium), has a Si/Al ratio about 2. In contrast, template-free synthesis leads to Si/Al =1 [32]. As results of increasing of Si/Al ration, thermal and chemical stability of the product will be improved remarkably.

Table 1: Chemical composition of the as-synthesized nano zeolite seed of LTA by Energy-Dispersive X-ray Spectroscopy (EDXS)

Element	Weight %	Atomic%
Oxygen	49,45	61,99
Sodium	9,03	7,88
Aluminum	16,15	12
Silicon	25,38	18,13
Si/Al	1,57	--
Total	100	100

4.2. Synthesis of zeolite composite substrate

4.2.1. *Synthesis Boehmite (γ-AlOOH)*

Boehmite nanoparticles were prepared by a peptization method in an aqueous nitric acid solution. Peptization is a process in which coagulated precipitates dissolve and recrystallize to form nanoparticles with an acid or base. Boehmite nanoparticles were characterized using powder X-ray diffraction and in-situ IR spectroscopy. The morphology of the nanoparticles obtained and deposited onto silicon dioxide wafer were characterized via Transmission Electron Microscopy and Scanning Electron Microscopy, respectively. Dynamic Light Scattering was used in order to obtain the particle size distribution in suspension.

In the formation of boehmite, aluminum tri-sec-butoxide $Al[OCH(CH_3)C_2H_5]_3$ is easily hydrolyzed with excess water because the water molecule is more nucleophilic than the alkoxyl group. Consequently, water molecules are formed by the reaction from the water molecules and the aluminum atoms in precursor. In our experiment, the hydrolysis reaction in acid was markedly expedited by the reaction temperature (90 °C) employed, giving rise to the formation of whitish boehmite nanoparticles.

The formation of boehmite from the hydrolysis of aluminum tri-sec-butoxide in acid may be sumarized as follows [33]

$$Al[OCH(CH_3)C_2H_5]_{3(l)} + (n+2)H_2O_{(l)} + HNO_3 \longrightarrow AlO(OH).H_2O_{(l)} + 3C_4H_9OH_{(g)}$$

Results obtained from DLS indicated a polydispersity sample with an average size of 80 nm and polidispersity of 0,22. A TEM observation indicates that the boehmite nanoparticles were about spherical in shape (Fig. 18a) and tended to form aggregated clusters with an apparent ‘‘particle’’ size in a range similar to that determined by the light-scattering method. The ‘‘real’’ particle size of boehmite may be in the 3 nm range. In contrast, figure 18(b) is an SEM micrograph of the boehmite solution prepared at pH 4. Particle

aggregation is apparent, suggesting a formation of continuous particulate network in the suspension structure.

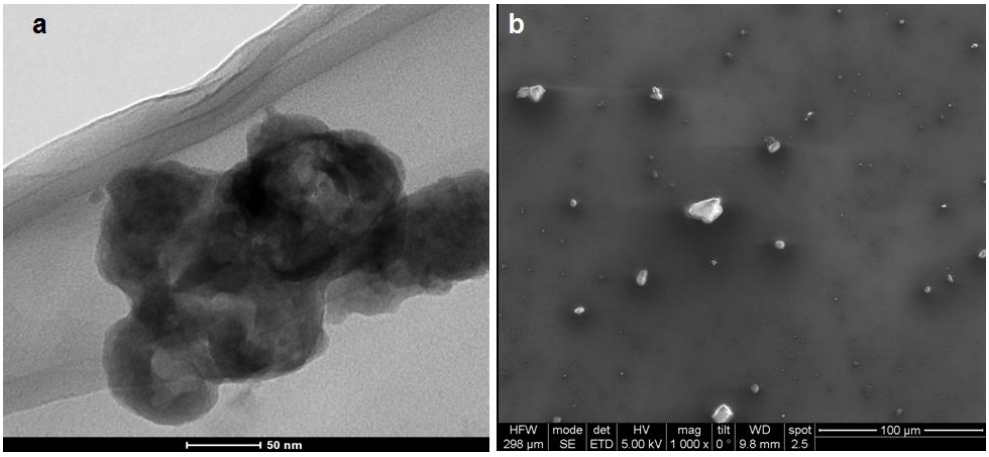

Figure 18. a) TEM image of boehmite nanoparticles synthesized from the $(Al(OCH(CH_3)_2)_3$ precursor in acid at 90 °C. b) SEM micrograph of seeded support with boehmite layer: (solution 9 wt% and pH 4)

Figure 19 show the infrared absorption spectra of the boehmite with 9 wt% of concentration before calcination at 600 °C. Typical bands for crystallized boehmite [34] can be observed: 3000 - 3600 cm^{-1} , O-H stretching vibrations; 1150 cm^{-1}, O-H bending vibrations; 1637 cm^{-1}, 1355 cm^{-1} , and 1078 cm^{-1} which can be assigned to Al=O, Al–O–H, and Al–O–Al bonds, respectively. The vibrations appear in the 3000-3600 cm^{-1} range as strong peaks are characteristic for -OH fragments of physisorbed water.

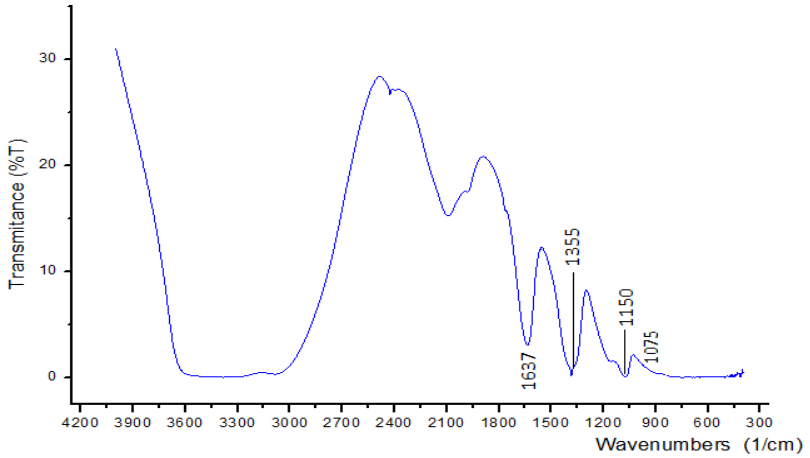

Figure 19. IR spectra of Boehmite measured in the range 4000 - 600cm^{-1} and a band resolution of 5 cm^{-1}.

The Boehmite synthesized was calcined (600°C during 6h) in order to get its dehydrated alumina form. The XRD pattern of the calcined sample (figure 20) indicates that a transformation form boehmite phase to γ-alumina after calcination occurred. All the peaks can be indexed to a cubic unit cell of γ-alumina (a = 7.900, b= 7.900, c= 7.900, JCPDS PDF No. 10-0425)

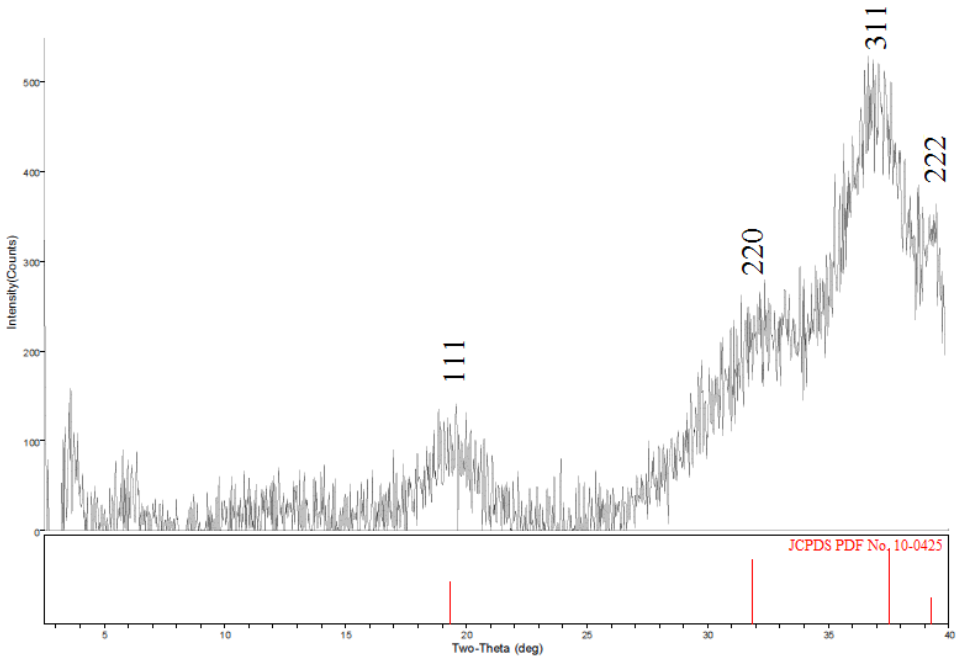

Figure 20. XDR patterns of the calcinated sample (black) and JCPDS card No. 10-0425 (red)

4.2.2. *Optimization of seeding process.*

The clean and modified silicon substrate was seeded using the procedure described in Section 3.2.2 in order to obtain a complete and uniform seed coverage. Different from the previous study, in the present work, the Boehmite was adsorbed on the support surface and was used to capture LTA zeolite particles during seeding process onto and subsequent ex situ hydrothermal synthesis. The main cause of crack of membrane layer was lack of good adherence between zeolite layer and substrate layer. As expecting the boehmite intermediate layer enhance the adherence between zeolite seed layer and substrate by hydrogen bonding. In the figure 21 is possible compare the zeolite seed (2 wt%) coating using PDDA and Boehmite as intermediate layer. The type of zeolite loading depended on

the coating of surface. Deposition parameters of PDDA layers reproduce the optimal conditions reported by previous work [30].

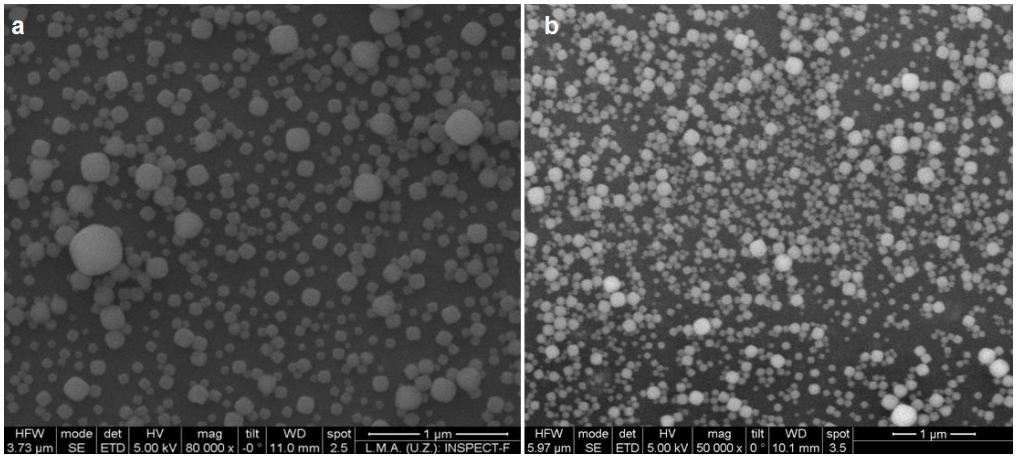

Figure 21. Zeolite seed coating using a) PDDA b) Boehmite, as an interlayer

The quality of the zeolite seed coating can be improved by employing the multi-stage coating methods such as is illustrated in the figure 22. The boehmite solution was spinned repeatedly on the silicon wafer in order to enhance zeolite seed coating. In all cases the zeolite seed solution (2 wt%) was spinned five times onto boehmite layer. Optimization of seeding process was carried out through the multi-stage coating methods and use of a boehmite interlayer.

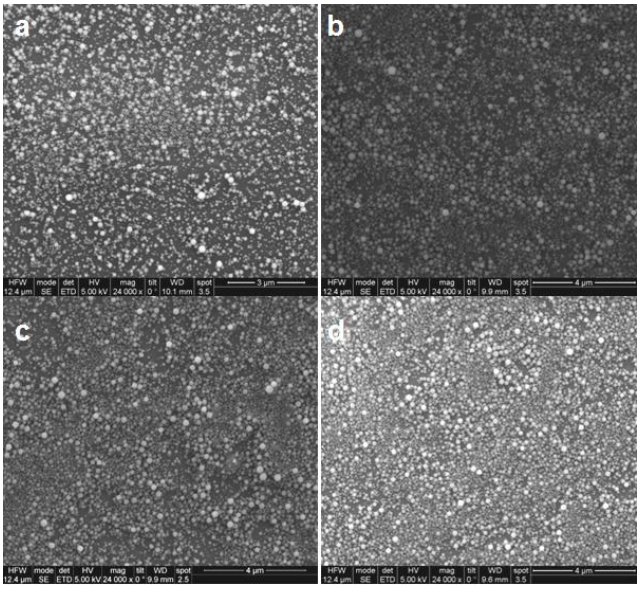

Figure 22. Multi-stage coating method: Boehmite solution (9 wt%) was spinned a) Once b) 3 times c) 5 times d) 8 times. Zeolite seed solution (1 wt%) was spinned 5 times onto silicon dioxide wafers.

Before the hydrothermal synthesis, the quality of zeolite seed layer on the microchannels structure were examined by scanning electron microscope. This is essential to check for imperfection in the zeolite layer which can result in formation of crack. Fabricated microchannel structures is shown in figure 23. The Zeolite A layer was uniform, compact and have a thickness of about~300 nm. It is important to note that prior to the sectioning of the sample for analysis with a scanning electron microscope, the zeolite film uniformly covers the entire substrate. Fig. 23 (a and b), show a top view and cross-section of microchannels fabricated onto the silicon substrate. In both samples, a~300 nm thick was observed. Initially the microchannels on silicon dioxide substrate were dipped into boehmite sol.

In the seeding process of microchannels, the size of the zeolite seed must be uniform and smaller than the channel width in order to prevent blockage and to ensure a uniform deposition. The zeolite loading can be controlled by changing the concentration of zeolite in the slurry and through repeated coating of the microchannel. The seed adhesion was strong and the zeolites remained onto substrate surface. Microchannels were dipped into boehmite solution (9 wt%) with a dipping speed of 0.1 mL/s and repeated 5 times. Following the substrate was dipped in a 1 wt% of A-type zeolite suspension in deionized water 5 times with same dipping speed.

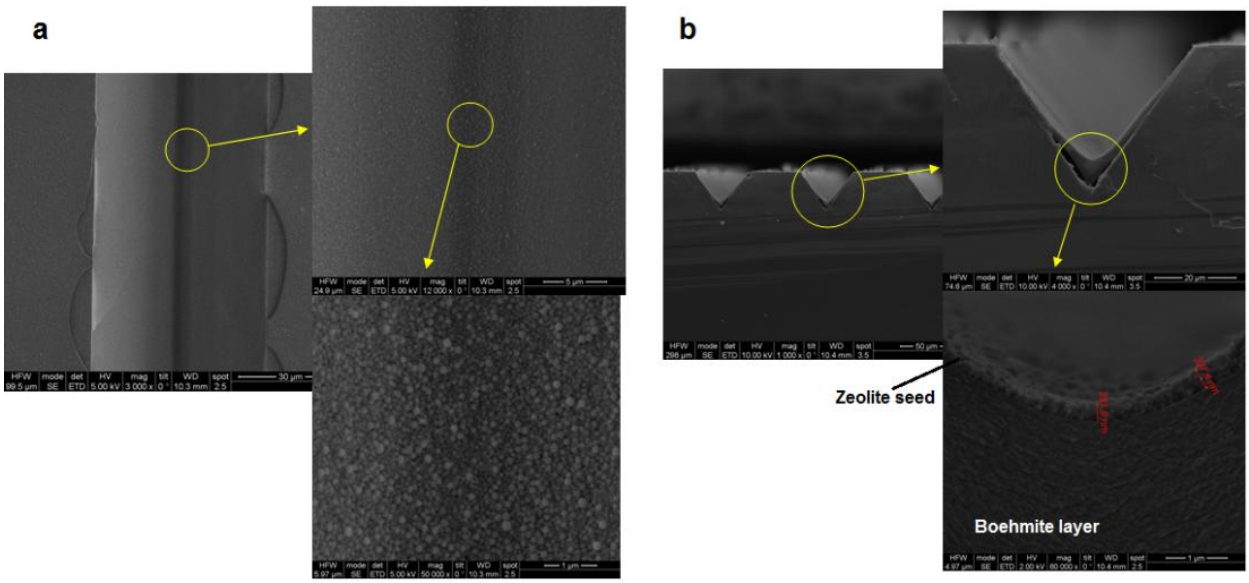

Figure 23. Scanning electron micrographs of seeding process microchannels on silicon substrates: (a) Top view (b) cross-section.

A cross section of the microchannel fabricated in SU-8 resin (Figure 24) shows the A-zeolite seed layer (1 wt %) deposited on the microchannel wall. The zeolite was uniformly deposited along the channel walls. The zeolite seed film displayed good adhesion to the channel but SU-8 resin was not able to withstand temperature treatments above 80°C without deforming of material substrate. The SU-8 support was modified with PDDA covalent linker at flow rate of 0.1 mL/min by 1 hour, changing the direction of flow for periods of 10 minutes. Then zeolite A was seeded with the same parameters of time and volumetric flow but at concentration of 1 wt%. .

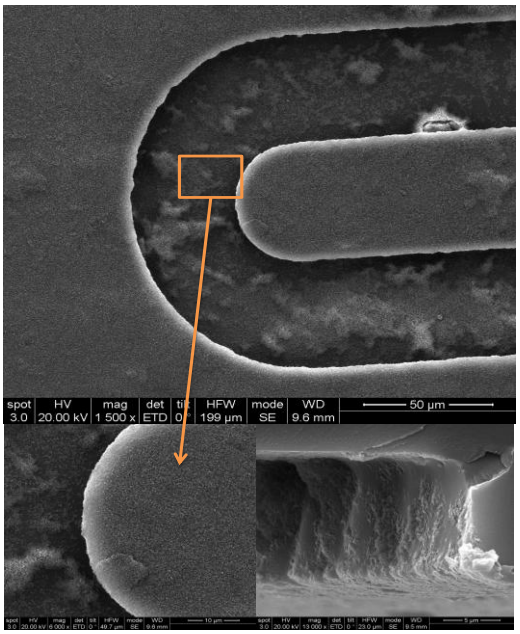

Figure 24. Scanning electron micrographs of seeding process microchannels on SU-8 support to mag x 1500, 6000 and 13000

4.2.3. *Hydrothermal Synthesis of layer A-type zeolite.*

The next step in the fabrication of zeolite-silicon composite substrate is hydrothermal synthesis. The seeding procedure involved the functionalization of the surface flat and 3D substrate with boehmite solution (9 wt%) utilizing different seeding

techniques (spin and Dip- coating) according type substrate. The composition of sol-gel precursor and parameter operating for hydrothermal synthesis are shown in the section 3.2.3. In order to obtain a high quality of zeolite intergrown onto substrates, synthesis time was evaluated. Six pieces of silicon dioxide wafer were modified with boehmite solution and seeded with zeolite nanocrystals. The seeding process steps was repeated such as written in section 3.2.2. A uniform and homogeneus zeolite seed coating, was obtained. A layer of zeolite was grown onto the seeded surfaces by placing the pieces of wafer horizontally in synthesis mixture contained in a teflon and with the molar composition is 2.8Na2O:2.7SiO2:1Al2O3:174-347H2O:0.05(TMA)2. The zeolite-silicon composite after the synthesis was rinsed in deionized water and dried in a plate heating at 150°C for 24 h. Scanning electron microscopy was used to examine the quality of the synthesis for crack-free zeolite layer. The figure 25 illustrates to result. The micrographs reveal that optimum time for hydrothermal synthesis was 12 hours (Fig 25d). The zeolite layers synthesized below this value (Fig 25a-c) have few thickness and above 12 hours the zeolite layer reveal cracks (Fig 25e,f).

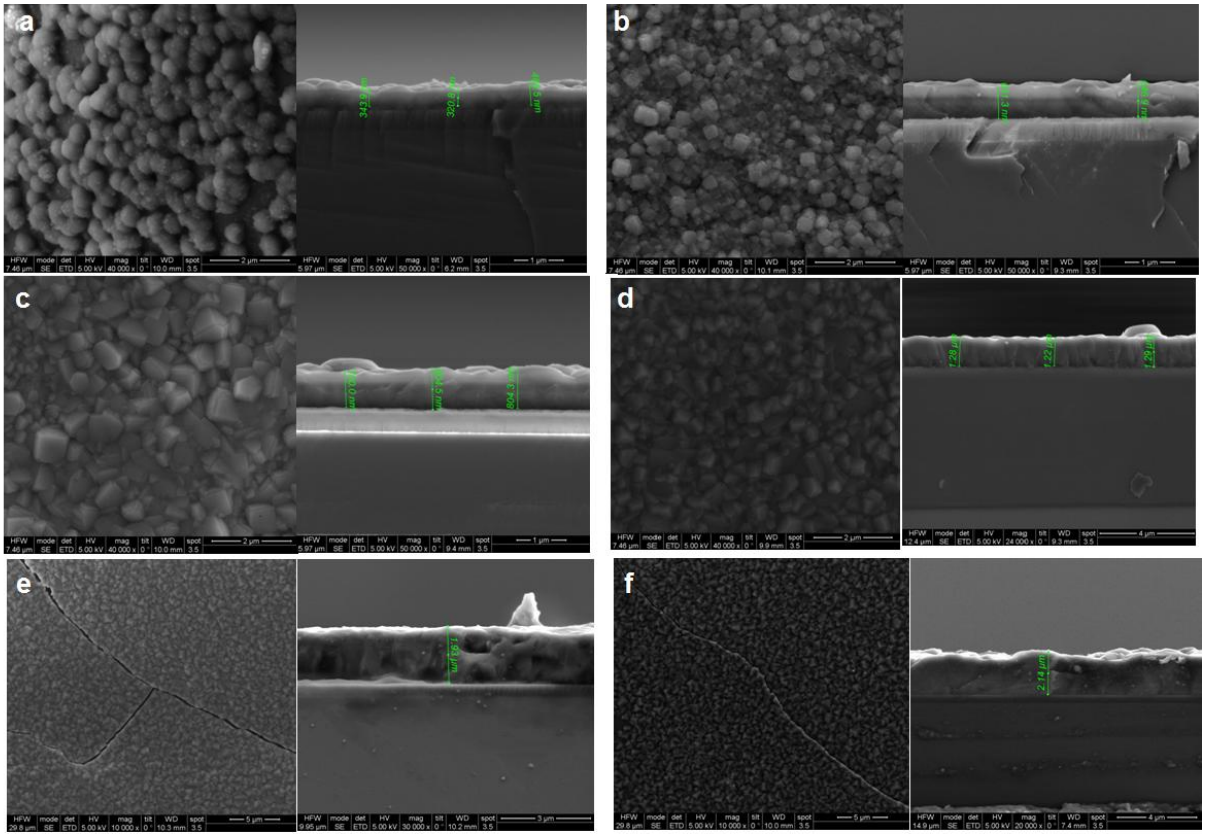

Figure 25. Micrographs (Top view and cross-section) of pieces wafer to different hydrothermal synthesis time. a) 5 h (~350 nm), b) 7 h (~ 650 nm), c) 9 h (~750 nm), d) 12 h (~1.5 µm), e) 15 h (~1.93µm), f) 20 h (~ 2.14 µm)

According to written above. The optimum conditions to obtain a layer of intergrown zeolite of high quality on flat substrates are summarized as follow. The silicon wafer with silicon dioxide layer was modified with a boehmite solution (9 wt%) utilizing spin-coating technique. The solution was spinned onto subtrate 8 times at pH 4. Then, support was dired to 200°C for 2 h. Following, seed zeolite A was spinned onto boehmite layer 5 times and finally dried to 150°C for 24 h. The angular speed used was initially 100 r.p.m by 1 minute, and then was spinned at 3000 r.p.m by 0.5 minute. Hydrothermal synthesis was carried out at 90°C by 12 hours. Figure 26 shows scale-up procedure for a 3 inch silicon wafers. The zeolite layer obtained have a thickness 1,5 µm and cracks-free.

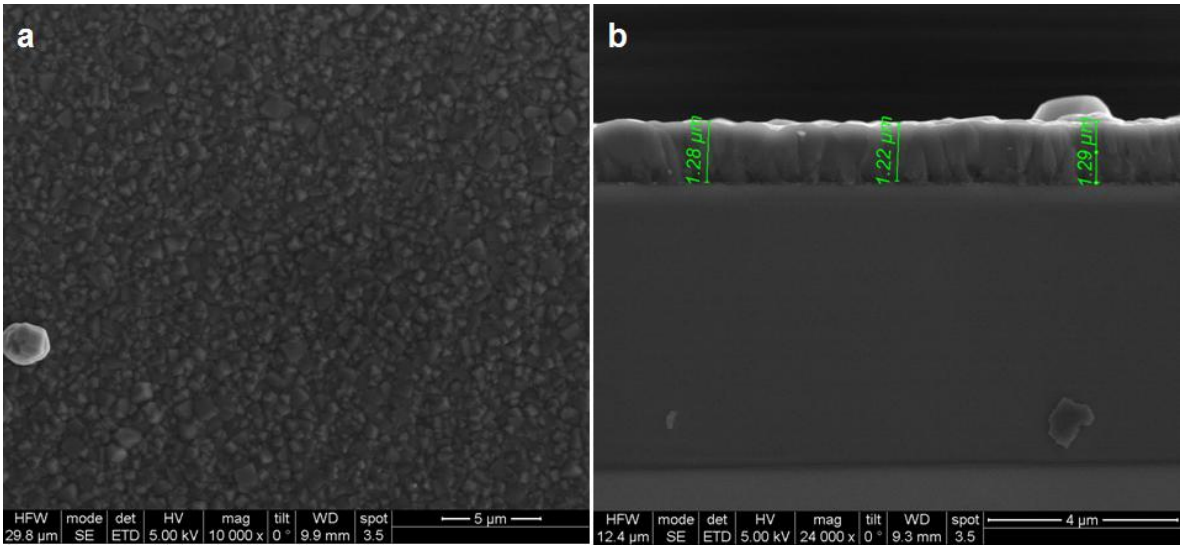

Figure 26. a) Top view and b) Cross-section image of A-type zeolite layer intergrown onto a 3 inch silicon dioxide wafer.

The figure 27 (a) and (b) show SEM image of top view and cross-section , respectively, of a high quality zeolite coatings intergrown on microchannel fabricated in silicon wafer. In this case, the dip-coating tecnique was preferred as seeding method. 3D substrate was dipped into boehmite solution (9 wt%) and A-type zeolite seed (1wt%) 5 times. The thickness of the films was similar as that for sample synthesized by 12 hours onto flat

substrate (Figure 25d). however, hydrothermal synthesis of microchannel was carried out at 90°C by 7,5 hours. The film seem to have continuous columnar morphology with single grains extending zoned regions. SEM imagen illustrated in figure 28b corresponds with image shown of seeding process in figure 21b.

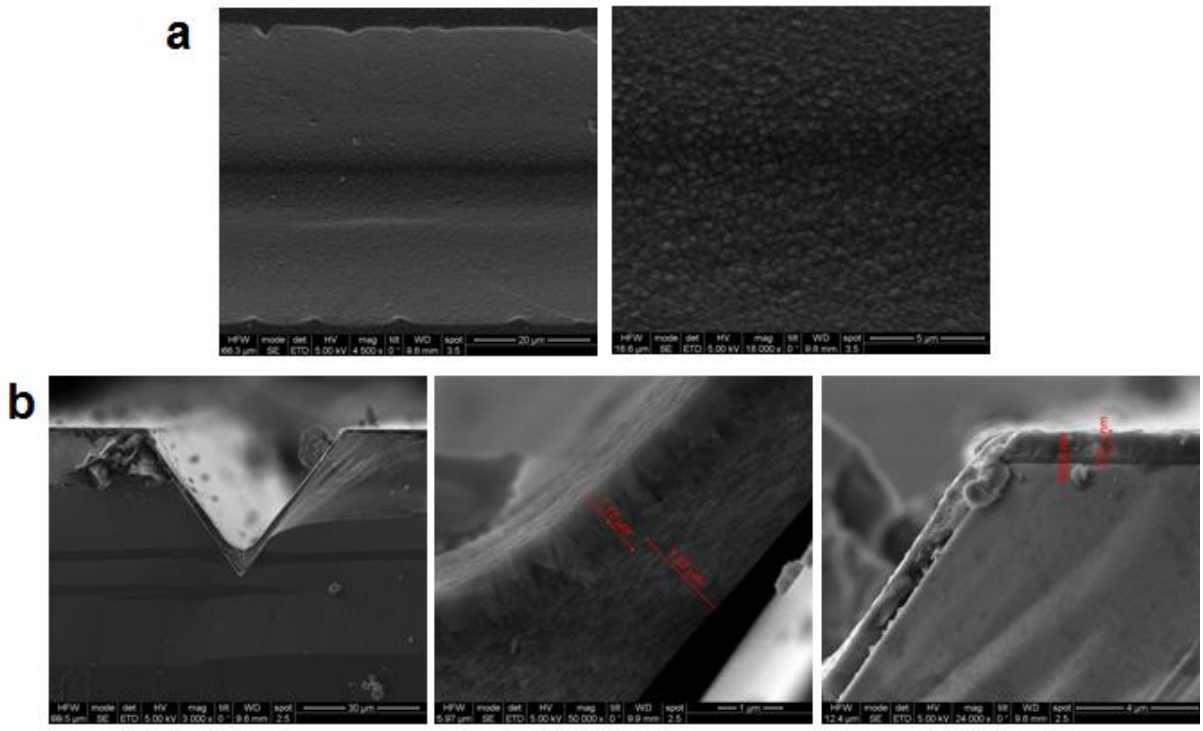

Figure 27. SEM image of the zeolite A layer on microchannel pattern obtained by hydrothermal synthesis at 90°C by 7.5 hours

4.2.3. *Elemental analysis of zeolite crystals (discrete and deposited form)*

Table 2 shows the comparison between composition of zeoite crystals synthesized without support (figure 28) and cross-section composition of zeolite film prepared in this work as measured by EDX. The discrete crystals has a Si/Al of 1.57. The average Si/Al ratio for film grown 2 um (Figure 25f) on silicon support with a interlayer of boehmite was 1.19. Both samples were calcinated at 480°C by 8 hours with rate ramp thermal of 1°C/min before analysis by EDX. These results indicated that after calcination the Si/Al ratio of zeolite film is lower that discrete crystals, this clearly shows that the aluminum

concentration increases at zeolite film, it is possible if aluminum migrates from the boehmite layer to the zeolite film during calcination.

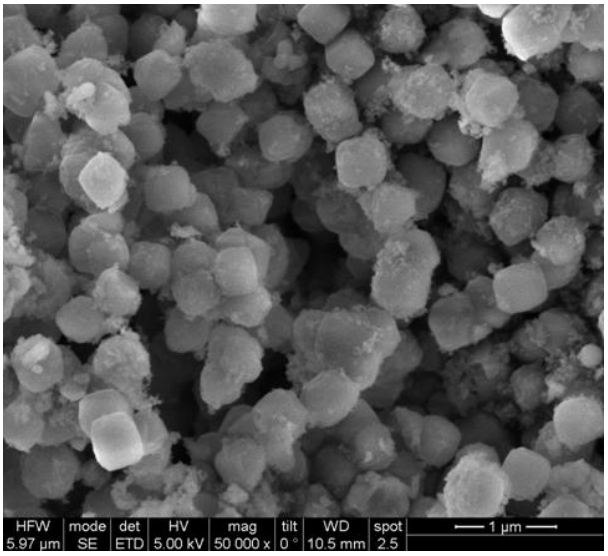

Figure 28. Discrete zeolite crystals obtained by hydrothermal synthesis without support to 90°C by 7.5 hours.

Table 2: Comparison between chemical composition of the as-synthesized zeolite crystal of LTA and zeolite film deposited on silicon substrate by Energy-Dispersive X-ray Spectroscopy (EDXS)

Zeolite Crystals			**Zeolite layer**		
Element	**Weight %**	**Atomic%**	**Element**	**Weight %**	**Atomic%**
Oxygen	49.80	62.26	Oxygen	44.43	55.31
Sodium	9.65	8.40	Sodium	31.58	27.36
Aluminum	15.95	11.83	Aluminum	10.93	8.07
Silicon	24.59	17.51	Silicon	13.05	9.26
Si/Al	**1.54**	**--**	**Si/Al**	**1.19**	**--**
Total	100	100	Total	100	100

On the other hand, the chemical composition of zeolite film intergrown onto silicon wafer was measured in different point of cross-section as such as is shown in table 3. Three

spectra were measured and the different points are illustrated in Figure 29. According to EDX, the Si/Al ratio near the surface of the film (Spectrum 1) and third point (spectrum 3) are similar, but in the second point, the Si/Al increases. These results indicate that silicon migrates from the silicon support to the surface of the zeolite film during the final calcination.

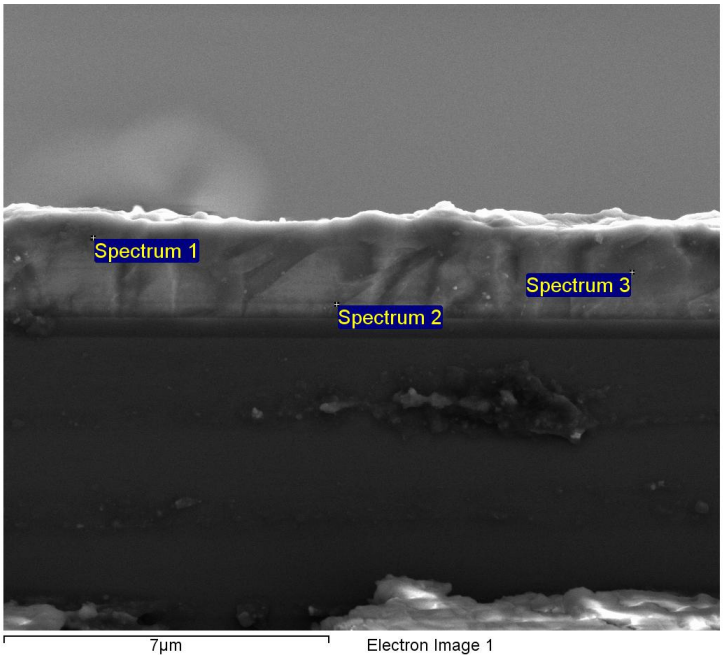

Figure 29. EDX analysis points on cross-section of zeolite layer intergrown onto silicon support synthesized to 90°C by 20 hours.

Table 3: Comparison Si/Al ratios measured by EDX, to different heights of A-type zeolite film (~2µm) deposited onto silicon dioxide substrate.

Element	Silicon	Aluminum	Si/Al
Spectrum 1	57.45	42.55	1.35
Spectrum 2	83.48	16.53	5.05
Spectrum 3	56.42	43.58	1.29

4.3. ADSORPTION /DESORPTION ANALYSIS.

REFERENCES

[1] **S. Auerbach.; Carrado, K.; Dutta, P**., *Handbook of zeolite science and technology*. Marcel Dekker Inc.: New York, 2003.

[2] **Bein, Thomas.,** *Synthesis and applications of molecular sieves layers and membranes.* American Chemical Society, 1996, Vol. 8.

[3] **Pellejero, Ismael.,** *Fabricación de microdispositivos basados en zeolitas y su aplicación en sensores y membranas*. Universidad de Zaragoza, 2011.

[4] **Gualtieri, Magdalena.,** *Synthesis and characterization of zeolite films and membranes*. University of Technology, Luleå, Sweden, 2006.

[5] **Kanna Aoki, Katsuki Kusakabe, Shigeharu Morooka**., *Gas permeation properties of A-type zeolite membrane formed on porous substrate by hydrothermal synthesis*. Journal of Membrane Science 141 (1998) 197-205.

[6] www.iza-structure.org/databases/, *Database of zeolite Structure*. Baerlocher Ch.

[7] **Jirí Cejka, Herman van Bekkum, Avelino Corma, Ferdi Schüth.** *Studies in surface science and catalysis 168 Introduction to zeolite sicience and practice.* ELSEVIER, 2007.

[8] 10**M. Urbiztondo, I. Pellejero, A. Rodriguez, M.P. Pina, J. Santamaria**., *Zeolite-coated interdigital capacitors for humidity sensing.* Sensors and Actuators B 157 (2011) 450– 459.

[9] 11**M.A. Urbiztondo, I. Pellejero, M. Villarroya, J. Sesé, M.P. Pina, I. Dufour, J. Santamaría**., *Zeolite-modified cantilevers for the sensing of nitrotoluene vapors*. Sensors and Actuators B 137 (2009) 608–616.

[10] 12**M.A. Urbiztondo, A. Peralta, I. Pellejero, J. Sesé, M.P. Pina, I. Dufour, J. Santamaría**. *Detection of organic vapours with Si cantilevers coated with inorganic (zeolites) or organic (polymer) layers.* Sensors and Actuators B 171– 172 (2012) 822– 831.

[11] **13M. Vilaseca, J. Coronas, A. Cirera, A. Cornet, J.R. Morante, J. Santamaria**., *Development and application of micromachined Pd/SnO_2 gas sensors with zeolite coatings*. Sensors and Actuators B 133 (2008) 435–441.

[12] **Castro Urbiztondo, Miguel**., *Microdispositivos basados en zeolitas: sensores y otras aplicaciones.* Universidad de Zaragoza, 2008.

[13] 27**Tai-Ran Hsu.,** *MEMS and microsystems: design and manufacture*. McGraw-Hill, Chapter 7. 2002.

[14] **J. Coronas, J. Santamaria**., *Separations with zeolite membranes*. Sep. Purif. Methods 28 (1999) 12–77.

[15] 17**Houda Lahlou**., *Design, fabrication and characterization of a gas preconcentrator based on thermal programmed adsorption/desorption for gas phase microdetection systems*. Universitat Rovira I Virgili, 2011.

[16] **H. Lahlou, X. Vilanova, X. Correig**., *Gas phase micro-preconcentrators for benzene monitoring: A review*. Sensors and Actuators B 176 (2013) 198– 210

[17] **Yehya Mohsen, Jean-Baptiste Sanchez, Franck Berger, Houda Lahlou, Igor Bezverkhyy, Vanessa Fierro, Guy Weber, Alain Celzard, Jean-Pierre Bellat**., *Selection and characterization of adsorbents for the analysis of an explosive-related molecule traces in the air.* Sensors and Actuators B 176 (2013) 124– 131

[18] **J. W. Russell**., *Analysis of Air Pollutants Using Sampling Tubes and Gas Chromatography*, Environmental Science & Technology 9 (1975) 1175-1178.

[19] **R. H. Brown**., *Collection and Analysis of Trace Organic Vapour Pollutants in Ambient Atmospheres: The Performace of a Tenax-Gc Adsorbent Tube.* Journal of Chromatography A 178 (1979) 79-90.

[20] **E. D. Pellizzar**., *Collection and Analysis of Trace Organic Vapor Pollutants in Ambient Atmospheres. The Performance of a Tenax GC Cartridge Sampler for Hazardous Vapors.* Analytical Letters 9 (1976) 45 - 63.

[21] **Lee, Jeong Hoon, and Jongyoon Han**., *Concentration-enhanced rapid detection of human chorionic gonadotropin as a tumor marker using a nanofluidic preconcentrator*. Microfluidics and Nanofluidics 9.4-5 (2010): 973-979.

[22] **I. Grácia, P. Ivanov, F. Blanco, N. Sabaté, X. Vilanova, X. Correig, L. Fonseca, E. Figueras, J. Santander, C. Cané**., *Sub-ppm gas sensor detection via spiral-preconcentrator.* Sensors and Actuators B 132 (2008) 149–154

[23] **Yehya Mohsen, Jean-Baptiste Sanchez, Franck Berger, Houda Lahlou, Igor Bezverkhyy, Vanessa Fierro, Guy Weber, Alain Celzard, Jean-Pierre Bellat**., *Selection and characterization of adsorbents for the analysis of an explosive-related molecule traces in the air*. Sensors and Actuators B 176 (2013) 124– 131

[24] **Rafal Szczypiński, Jacek Grzelka, Anna Baraniecka, Marianna Górska, Jan Lesiński, Jan Łysko, Remigiusz Grodecki, Dorota G. Pijanowska, Piotr Grabiec**., *Microfluidic preconcentrator and microfluidic chip for bacterial cells detection.* Optica Applicata, Vol. XLI, No. 2, 2011

[25] **S. Mitra and C. Yun**., *Continuous gas chromatographic monitoring of low concentration sample streams using an on-line microtrap.* J. Chromatogr. A (1993), 648, 415-421

[26] **F. Blanco**., *Fabrication and characterisation of microporous activated carbon-based preconcentrators for benzene vapou*rs. Sensors and Actuators B 132 (1) (2008) 90-98.

[27] **C. Pijolat**., *Application of Carbon Nano-Powders for a Gas Micro-Preconcentrator*. Sensors and Actuators B: Chemical 127 (2007) 179-185.

[28] **Williams JD, Wang W.,** *Using megasonic development of SU-8 to yield ultra-high aspect ratio microstructures with UV lithography*. Microsyst Technol (2004) 10(10): 694–698

[29] **Colin S. Cundy, Paul A. Cox**., *Review: The hydrothermal synthesis of zeolites: Precursors, intermediates and reaction mechanism*. Microporous and Mesoporous Materials 82 (2005) 1–78.

[30] **Luaces Orobitg, Susana M**., *Development of zeolite-silicon composites to be used as substrates in microfabrications applications*. Universidad de Zaragoza, 2011

[31] **B. E. Yoldas.,** *Alumina Sol Preparation from Alkoxides*. American Ceramic Society Bulletin 54, 3 (1975), 289-290.

[32] **Bouizi Y., Paillaud J. L., Simon L., Valtchev V.,** *Seeded Synthesis of Very High Silica Zeolite A,* Chem. Mater., 19 (2007) 652 -653

[33] **M. Nguefack, A.F. Popa, S. Rossignol, C. Kappenstein**., *Preparation of alumina through a sol-gel process. Synthesis, characterization, thermal evolution and model of intermediate boehmite,* Phys. Chem. Chem. Phys. 5 (2003) 4279–4289.

[34] Mahdi Mirzaee, Mostafa M. Amini, Mahdi Sadeghi, Farnaz Yeganeh Mousavi, Maasomeh Sharbatdaran., Preparation and characterization of boehmite, CuO, TiO_2 and Nb_2O_5 by hydrothermal assisted sol-gel processing of metal alkoxides. Ceramics − Silikáty 49 (1) 40-47 (2005)

[28] **Wen Dai, Kun Lian, Wanjun Wang**. *A quantitative study on the adhesion property of cured SU-8 on various metallic surfaces*. Microsyst Technol (2005) 11: 526–534.

[30] **Seidemann V**. *A novel fabrication process for 3D meander shaped micro coils in SU8 dielectric and their application to linear micro motors*. Proc SPIE Conf on Microelectronics and MEMS Technologies, SPIE 4407: (2001) 304-309

[31] **Zhang J; Tan KL; Hong GD; Yang LJ; Gong HQ.** *Polymerization optimization of SU-8 photoresist and its applications in microfludic systems and MEMS*. J Micromech Microeng (2001) 11:20-26

[32] **Lin CH; Lee GB; Chang BW; Chang GL.** *A new fabrication process for ultra-thick microfluidic microstructures utilizing SU-8 photoresist.* J Micromech Microeng 12 (2002) 590-597

[33] **Nandini Das, Debtosh Kundu, Minati Chatterjee**., *The effect of intermediate layer on synthesis and gas permeation properties of NaA zeolite membrane*. J. Coat. Technol. Res., 7 (3) 383–390, 2010